Title	Flow of an Inviscid Fluid past an Axially Symmetrical Body in a Tube for Various Upstream Conditions
Author(s)	Minami, Kenji; Nakatani, Hitoshi; Miyai, Yoshihiro
Editor(s)	
Citation	Bulletin of University of Osaka Prefecture. Series A, Engineering and natural sciences. 1972, 21(1), p.15-25
Issue Date	1972-09-30
URL	http://hdl.handle.net/10466/8191
Rights	

Flow of an Inviscid Fluid past an Axially Symmetrical Body in a Tube for Various Upstream Conditions

Kenji MINAMI, *Hitoshi NAKATANI** and Yoshihiro MIYAI**

(Received June 13, 1972)

The stream functions for a few doubulets have been derived respectively for the case of axially symmetrical, inviscid and incompressible flow in an infinitely long tube of constant diameter, when the far upstream flow is the following different types of flow; (1) irrotational flow, (2) rotational flow with a paraboloidal velocity distribution and velocity distribution attributed to the law of 1/7 power.

Stream lines including a stagnation streamline for each far upstream flow have been calculated with the above stream functions. And also, pressure coefficients on the bodies which are constituted by the stagnation streamlines have been evaluated.

1. Introduction

The analysis of flow of an inviscid, incompressible fluid past an axially symmetrical body on the axis of a tube is very complicated in the analysis because of difficulty of solving the integral equation which has unknown functions of the strength of sources, sinks or doublets in the case that the shape of body is given.

In this paper, as a first step, it is a purpose that we examine how the shapes of bodies are formed by changing the upstream condition and how the flows are changed by the influence of a tube wall in the case that a few doublets exist along the tube axis.

The following two differential types of flow are considered;

(1) irrotational flow, that is, uniform florm far upstream

(2) rotational flow, that is, the flow with paraboloidal velocity distribution and the velocity distribution attributed to the law of 1/7 power far upstream.

2. Theoritical Analysis

Cylindrical co-ordinates (r, θ, z) will be used. In these co-ordinates, the velocity components will be denoted by u, v and w, respectively.

At first, we wish to investigate the case of axially symmetrical flow of a steady, inviscid, incompressible potential fluid inside a circular tube.

The differential equation for the velocity potential is well known, and may be written as

$$\Phi_{rr}+(1/r)\Phi_r+\Phi_{zz}=0. \tag{1}$$

* Graduate student, Department of Mechanical Engineering, College of Engineering.

** Department of Mechanical Engineering, College of Engineering.

Consider a source of strength $4\pi m$, located at $z=r=0$ as shown in Fig. 1.

The velocity potential Φ, as given by Philip Levine,[1] is

$$\Phi = \pm 2mz - 2m\sum_{n=1}^{\infty} \frac{e^{-j_n|z|}}{j_n J_0^2(j_n)} J_0(j_n r), \tag{2}$$

where the values of (j) are the n-th ordered roots of J_1. J_1 is the Bessel function of the first kind of first order. J_0 is the Bessel function of the first kind of 0-th order.

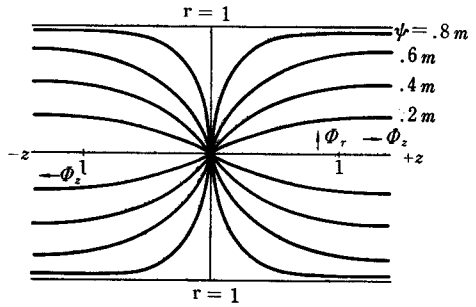

Fig. 1. Coordinate system and streamlines of a point source.

To derive the velocity potential for a doublet, we have only to place a source and sink of the same strength a small distance apart on the axis, and find the resultant potential under the condition that

$$M = \lim_{\Delta z \to 0} m\Delta z,$$

where M is the strength of the doublet. The velocity potential for a doublet is obtained. And the Stokes stream function[1] corresponding to it is

$$\Psi = -2Mr\sum_{n=1}^{\infty} \frac{e^{-j_n|z|}}{J_0^2(j_n)} J_1(j_n r). \tag{3}$$

Next, we wish to investigate the case of rotational flow. In this case, according to Wei Lai[2] and G. K. Batchelor,[3] the governing equation in the cases that are irrotational flow, swirling flow and rotational flow far upstream is

$$\frac{\partial^2\Psi}{\partial z^2} + \frac{\partial^2\Psi}{\partial r^2} - \frac{1}{r}\frac{\partial\Psi}{\partial r} = r^2\frac{dH}{d\Psi} - \frac{1}{2}\frac{df}{d\Psi}, \tag{4}$$

where $f(\Psi) = (rv)^2$, $H(\Psi) = \frac{1}{2}(u^2+v^2+w^2) + (P/\rho) + \Omega$, P is a pressure, ρ is a (constant) density, Ω is the potential of external forces (gravity). $H(\Psi)$ and $f(\Psi)$ are to be determined from the conditions far upstream.

As shown in Fig. 2, the upstream conditions are characterized by

(I) $\quad w = W_u (=\text{constant}), \quad u = v = 0, \tag{5}$

(II) $\quad w = W_s(1-r^2), \quad u = v = 0, \tag{6}$

(III) $\quad w = W_k(1-r^2)^{1/7}, \quad u = v = 0, \tag{7}$

where the radius of a circular tube is unity. We call the above flows uniform flow, shear

flow and Karman flow, respectively.

The Stokes stream functions corresponding to these velocity distributions are

(I) $$\Psi=\frac{1}{2}r^2W_u, \tag{8}$$

(II) $$\Psi=\left(\frac{1}{2}r^2-\frac{1}{4}r\right)W_s, \tag{9}$$

(III) $$\Psi=-\frac{7}{8}r(1-r)^{8/7}W_k-\frac{49}{120}(1-r)^{15/7}W_k, \tag{10}$$

respectively.

The following Stokes stream functions (11)～(16), as suggested by Wei Lai[2] and G. K. Batchelor,[3] are derived by using (3) and (8)～(10). And these Stokes stream functions (11)～(16) satisfy with the governing equation (4).

$$\Psi=\frac{1}{2}r^2W_u-2Mr\sum_{n=1}^{\infty}\frac{e^{-j_n|z|}}{J_0^2(j_n)}J_1(j_nr), \tag{11}$$

$$\Psi=\frac{1}{2}r^2W_s-\frac{1}{4}r^4W_s-2Mr\sum_{n=1}^{\infty}\frac{e^{-j_n|z|}}{J_0^2(j_n)}J_1(j_nr), \tag{12}$$

$$\Psi=-\frac{7}{8}r(1-r)^{8/7}W_k-\frac{49}{120}(1-r)^{15/7}W_k-2Mr\sum_{n=1}^{\infty}\frac{e^{-j_n|z|}}{J_0^2(j_n)}J_1(j_nr), \tag{13}$$

$$\Psi=\frac{1}{2}r^2W_u-2Mr\sum_{n=1}^{\infty}\frac{e^{-j_n|z|}}{J_0^2(j_n)}J_1(j_nr)-2Mr\sum_{n=1}^{\infty}\frac{e^{-j_n|z-a|}}{J_0^2(j_n)}J_1(j_nr), \tag{14}$$

$$\Psi=\frac{1}{2}r^2W_s-\frac{1}{4}r^4W_s-2Mr\sum_{n=1}^{\infty}\frac{e^{-j_n|z|}}{J_0^2(j_n)}J_1(j_nr)-2Mr\sum_{n=1}^{\infty}\frac{e^{-j_n|z-a|}}{J_0^2(j_n)}J_1(j_nr), \tag{15}$$

$$\Psi=-\frac{7}{8}r(1-r)^{8/7}W_k-\frac{49}{120}(1-r)^{15/7}W_k-2Mr\sum_{n-1}^{\infty}\frac{e^{-j_n|z|}}{J_0^2(j_n)}J_1(j_nr)-2Mr\sum_{n=1}^{\infty}\frac{e^{-j_n|z-a|}}{J_0^2(j_n)}J_1(j_nr). \tag{16}$$

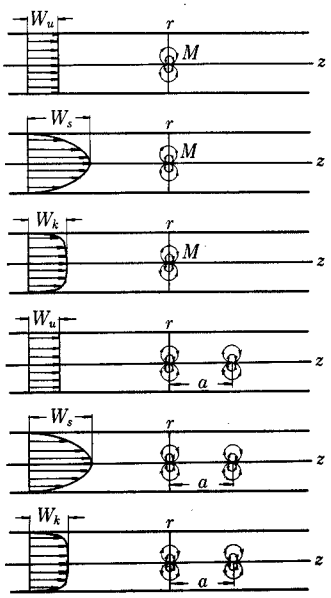

Fig. 2. Relations between upstream conditions and doublet distribution, where W_u, W_s and W_k are the maximum velocities in uniform flow, shear flow and Karman flow respectively.

In equations (11)～(13), a doublet of stength M, as shown in Fig. 2, is located at $z=r=0$. And in equations (14)～(16), one doublet of strength M is located at $z=r=0$, the other of strength M is located at $z=a$, $r=0$.

In order to compare easily with each stream lines of equations (11)～(16), Stokes stream functions Ψ^* of equations (17)～(22) are normalized by the mean velocity of fluid U_m, which is unity, so as to be $\Psi^*=0.5$ at tube wall. ($r=R=1$)

$$(\mathrm{I}) \quad \Psi^*=\frac{1}{2}r^2-2\frac{M}{U_m}r\sum_{n=1}^{\infty}\frac{e^{-j_n|z|}}{J_0^2(j_n)}J_1(j_nr), \tag{17}$$

$$(\mathrm{II}) \quad \Psi^*=r^2-\frac{1}{2}r^4-2\frac{M}{U_m}r\sum_{n=1}^{\infty}\frac{e^{-j_n|z|}}{J_0^2(j_n)}J_1(j_nr), \tag{18}$$

$$(\mathrm{III}) \quad \Psi^*=-\frac{15}{14}r(1-r)^{8/7}-\frac{1}{2}(1-r)^{15/7}-2\frac{M}{U_m}r\sum_{n=1}^{\infty}\frac{e^{-j_n|z|}}{J_0^2(j_n)}J_1(j_nr)+0.5, \tag{19}$$

$$(\mathrm{I})' \quad \Psi^*=\frac{1}{2}r^2-2\frac{M}{U_m}r\sum_{n=1}^{\infty}\frac{e^{-j_n|z|}}{J_0^2(j_n)}J_1(j_nr)-2\frac{M}{U_m}r\sum_{n=1}^{\infty}\frac{e^{-j_n|z-a|}}{J_0^2(j_n)}J_1(j_nr), \tag{20}$$

$$(\mathrm{II})' \quad \Psi^*=r^2-\frac{1}{2}r^4-2\frac{M}{U_m}r\sum_{n=1}^{\infty}\frac{e^{-j_n|z|}}{J_0^2(j_n)}J_1(j_nr)-2\frac{M}{U_m}r\sum_{n=1}^{\infty}\frac{e^{-j_n|z-a|}}{J_0^2(j_n)}J_1(j_nr), \tag{21}$$

$$(\mathrm{III})' \quad \Psi^*=-\frac{15}{14}r(1-r)^{8/7}-\frac{1}{2}(1-r)^{15/7}-2\frac{M}{U_m}r\sum_{n=1}^{\infty}\frac{e^{-j_n|z|}}{J_0^2(j_n)}J_1(j_nr)-2\frac{M}{U_m}r\sum_{n=1}^{\infty}\frac{e^{-j_n|z-a|}}{J_0^2(j_n)}J_1(j_nr)+0.5. \tag{22}$$

Then the pressure coefficient C_p is derived from the following equation,

$$C_p=\frac{P-P_\infty}{\frac{1}{2}\rho U_\infty^2}=1-\left(\frac{U}{U_\infty}\right)^2=1-\frac{1}{U_\infty^2}\left\{\left(-\frac{1}{r}\frac{\partial\Psi^*}{\partial z}\right)^2+\left(\frac{1}{r}\frac{\partial\Psi^*}{\partial r}\right)^2\right\}. \tag{23}$$

The equations of C_p corresponding to (I)～(III) and (I)′～(III)′ are

$$C_p=1-\left[\left(1-2\frac{M}{U_m}\sum_{n=1}^{\infty}\frac{e^{-j_n|z|}}{J_0^2(j_n)}j_nJ_0(j_nr)\right)^2+4\frac{M^2}{U_m^2}\left(\sum_{n=1}^{\infty}\frac{e^{-j_n|z|}}{J_0^2(j_n)}j_nJ_1(j_nr)\right)^2\right], \tag{24}$$

$$C_p=1-\left[\left(1-r^2-\frac{M}{U_m}\sum_{n=1}^{\infty}\frac{e^{-j_n|z|}}{J_0^2(j_n)}j_nJ_0(j_nr)\right)^2+\frac{M^2}{U_m^2}\left(\sum_{n=1}^{\infty}\frac{e^{-j_n|z|}}{J_0^2(j_n)}j_nJ_1(j_nr)\right)^2\right], \tag{25}$$

$$C_p=1-\left(\frac{49}{60}\right)^2\left[\left(\frac{60}{49}(1-r)^{1/7}-2\frac{M}{U_m}\sum_{n=1}^{\infty}\frac{e^{-j_n|z|}}{J_0^2(j_n)}j_nJ_0(j_nr)\right)^2+4\frac{M^2}{U_m^2}\left(\sum_{n=1}^{\infty}\frac{e^{-j_n|z|}}{J_0^2(j_n)}j_nJ_1(j_nr)\right)^2\right], \tag{26}$$

$$C_p=1-\left[\left(1-2\frac{M}{U_m}\sum_{n=1}^{\infty}\frac{e^{-j_n|z|}}{J_0^2(j_n)}j_nJ_0(j_nr)-2\frac{M}{U_m}\sum_{n=1}^{\infty}\frac{e^{-j_n|z-a|}}{J_0^2(j_n)}j_nJ_0(j_nr)\right)^2+4\frac{M^2}{U_m^2}\left(\sum_{n=1}^{\infty}\frac{e^{-j_n|z|}}{J_0^2(j_n)}j_nJ_1(j_nr)+\sum_{n=1}^{\infty}\frac{e^{-j_n|z-a|}}{J_0^2(j_n)}j_nJ_1(j_nr)\right)^2\right], \tag{27}$$

$$C_p=1-\left[\left(1-r^2-\frac{M}{U_m}\sum_{n=1}^{\infty}\frac{e^{-j_n|z|}}{J_0^2(j_n)}j_nJ_0(j_nr)-\frac{M}{U_m}\sum_{n=1}^{\infty}\frac{e^{-j_n|z-a|}}{J_0^2(j_n)}j_nJ_0(j_nr)\right)^2\right.$$
$$\left.+\frac{M^2}{U_m^2}\left(\sum_{n=1}^{\infty}\frac{e^{-j_n|z|}}{J_0^2(j_n)}j_nJ_1(j_nr)+\sum_{n=1}^{\infty}\frac{e^{-j_n|z-a|}}{J_0^2(j_n)}j_nJ_1(j_nr)\right)^2\right], \tag{28}$$

$$C_p=1-\left(\frac{49}{60}\right)^2\left[\left(\frac{60}{49}(1-r)^{1/7}-2\frac{M}{U_m}\sum_{n=1}^{\infty}\frac{e^{-j_n|z|}}{J_0^2(j_n)}j_nJ_0(j_nr)\right.\right.$$
$$\left.-2\frac{M}{U_m}\Sigma\frac{e^{-j_n|z-a|}}{J_0^2(j_n)}j_nJ_0(j_nr)\right)^2+4\frac{M^2}{U_m^2}\left(\sum_{n=1}^{\infty}\frac{e^{-j_n|z|}}{J_0^2(j_n)}j_nJ_1(j_nr)$$
$$\left.+\sum_{n=1}^{\infty}\frac{e^{-j_n|z-a|}}{J_0^2(j_n)}j_nJ_1(j_nr)\right)^2\right]. \tag{29}$$

The values of C_p are derived from Bernoulli's equation along the stagnation streamline so that the maximum velocities of uniform flow, shear flow and Karman flow are 1, 2 and 60/49, respectively.

3. Numerical Results of Stokes Streamlines and of Pressure Distributions

Streamlines Ψ^* and pressure coefficients C_p are calculated for several kinds of M/U_m and of upstream conditions which are shown in Table 1.

Table 1. Upstream conditions, doublet strength M/U_m and distance a/R between two doublets.

(A) The case of one doublet

	Flow type	M/U_m		
I	Uniform flow	0.5	1.0	2.0
II	Shear flow	0.5	1.0	2.0
III	Karman flow	0.5	1.0	2.0

(B) The case of two doublets

	Flow type	M/U_m		
I	Uniform flow	0.25	0.5	1.0
II	Shear flow	0.25	0.5	1.0
III	Karman flow	0.25	0.5	1.0

where a/R=const.

	Flow type	a/R	
I	Uniform flow	1.0	1.5
II	Shear flow	1.0	1.2
III	Karman flow	1.0	1.5

where M/U_m=const.

A few calculating results of flow patterns and pressure distributions are shown in Figs. (3)～(11).

The one-fourth of tube axis-wise section is shown in these Figs. (3)～(11). The curve with arrows on the stagnation streamline shows the distribution of C_p on it. The streamlines of far upstream condition of each type flow are shown on the left of the tube axis-wise section in these figures.

(A) The case of one doublet

Figure 3 is the case of uniform flow far upstream and of the doublet strength M/U_m =1.0.

C_p equals to unity at stagnation point, and the minimum value of C_p is about -20.0 at $z=0$.

Figure 4 is the case of shear flow far upstream and the same doublet strength to uniform flow. It is found that a shape of stagnation streamline is smaller than in the case of uniform flow. The minimum value of C_p is about -4.0 at the center of the body which is formed by a stagenation streamline, and the value is considerably higher than that of uniform flow.

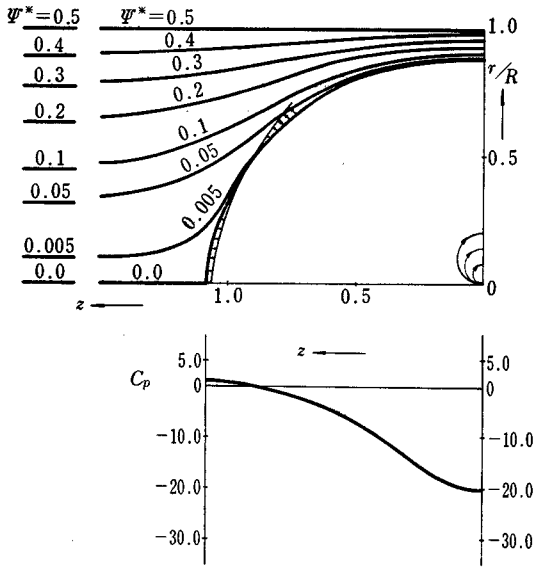

Fig. 3. Uniform flow $M/U_m=1.0$, $a/R=0.0$.

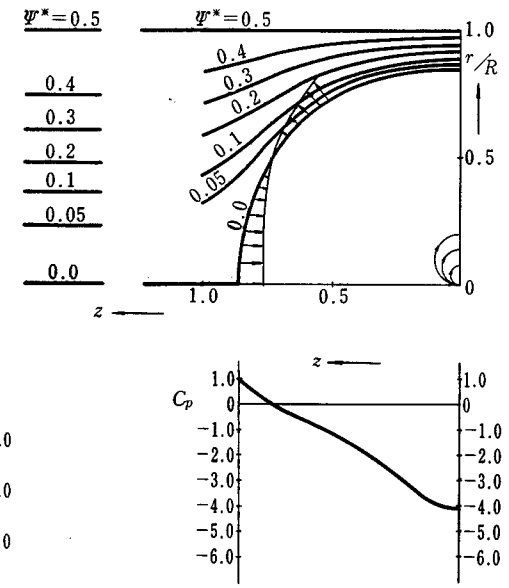

Fig. 4. Shear flow $M/U_m=1.0$, $a/R=0.0$.

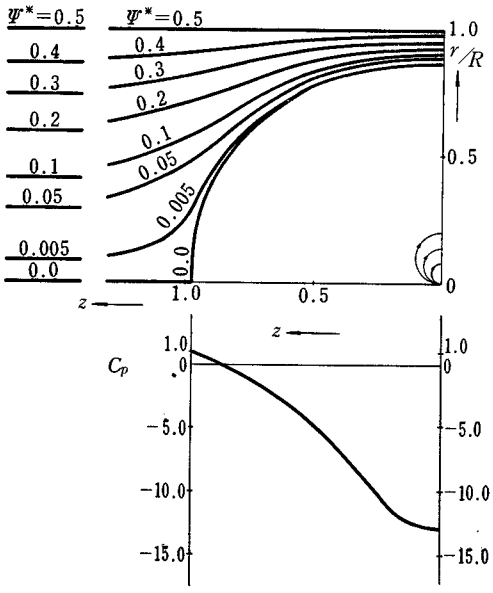

Fig. 5. Karman flow $M/U_m=1.0$, $a/R=0.0$.

Figure 5 is the case of Karman flow far upstream and of the same doublet strength as the above case. In this case, the flow pattern and the distribution of C_p show intermediate value of the above two cases, and the minimum value of C_p is about -13.0 at $z=0$. In the above three cases, the stagnation streamlines stretch along z-axis according to increase of the doublet strength because of the affection of tube wall. Inversely, they become nearly sphere according to decrease of the doublet strength, and in that case, particular when $M/U_m<0.5$, it is clear that the affection of tube wall is almost negligible.

(B) The case of two doublets

Figure 6 is the case of uniform flow far upstream and of two doublets. The strength M/U_m of both doublets equals to 0.25 respectively and the distance between two doublets a/R is 0.5 (R: tube radius). Under this condition of doublet strength, the stagnation streamline will be nearly sphere in the case of one doublets, but in this case, it stretches along z-axis owing to two doublets. Minimum value of C_p along the stagnation streamline is about -6.4 at $z=0$.

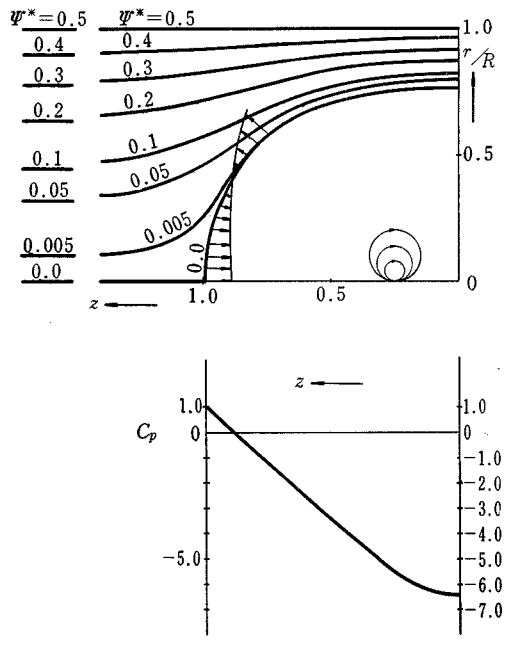

Fig. 6. Uniform flow $M/U_m=0.25$, $a/R=0.5$.

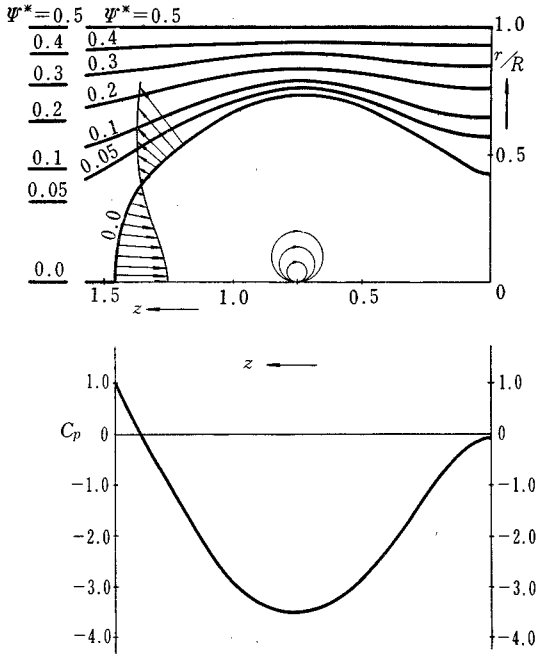

Fig. 7. Uniform flow $M/U_m=0.25$, $a/R=1.5$.

Figure 7 is the case of uniform flow far upstream and of two doublets. The strength M/U_m equals to 0.25 respectively and the distance a/R is 1.5. The r-component along the stagnation streamline has maximum value at $z=0.75$, and it decreases up to $z=0$. The value of C_p decreases rapidly from $C_p=1.0$ at stagnation point to about $C_p=-3.5$ at $z=0.75$, and it increases from $z=0.75$ to $z=0$ where C_p is almost null.

Figure 8 is the case of shear flow far upstream and of two doublets. The strength M/U_m equals to 0.25 respectively and a/R is 0.5. In this case, the affection of existing

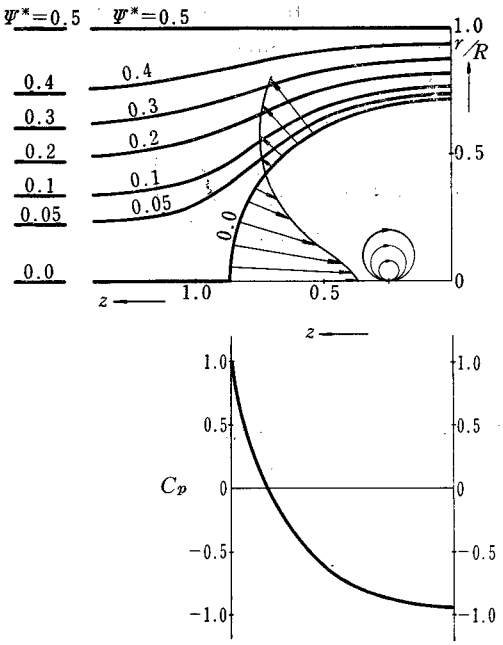

Fig. 8. Shear flow $M/U_m=0.25$, $a/R=0.5$.

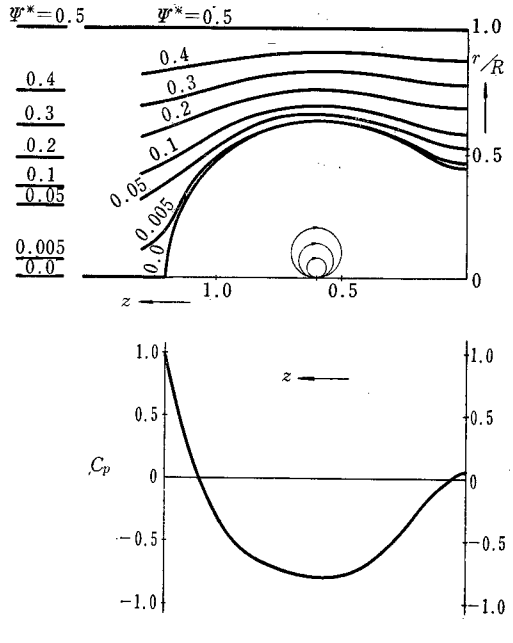

Fig. 9. Shear flow $M/U_m=0.25$, $a/R=1.2$.

two doublets does not appear so clearly. The value of C_p is about -0.9 at $z=0$.

Figure 9 is the case of shear flow far upstream and of two doublets. The strength M/U_m equals to 0.25 respectively and a/R is 1.2. In general, flow quantity is much in the vicinity of z-axis in shear flow, and also its feature appears in this case. At $z=0$, the value of C_p is almost 0.1.

Figure 10 is the case of Karman flow far upstream and of two doublets. The doublet strength M/U_m equals to 0.25 respectively and a/R is 0.5. It would be seen that the flow field in this case is similar to that in the case of uniform flow with same condition as this case.

Figure 11 is the case of Karman flow far upstream and of two doublets. The strength M/U_m equals to 0.25 respectively and a/R is 1.5. The radius of the body at $z=0$ is smaller than the one of uniform flow with same condition as this case, and the value of C_p is about -0.3 at $z=0$.

In Figs. (6)～(11), the value of the radius of the body at $z=0$ becomes small as the distance a/R between two doublets increases. We see the above facts in Figs. (7), (9) and (11). And at the case of $a/R=3.0$ for all upstream conditions, it is found by our calculation that the stagnation streamline forms separate two body shapes around each doublet. The facts derived from the observation of the shapes of the stagenation streamlines are as follows: The shapes in the case of uniform flow or Karman flow are generally larger than those in the case of shear flow. In other words the shapes in the former cases are more affected, by doublets rather than upstream condition, than those in latter case. And in the case of uniform flow and Karman flow, both flow patterns are almost same.

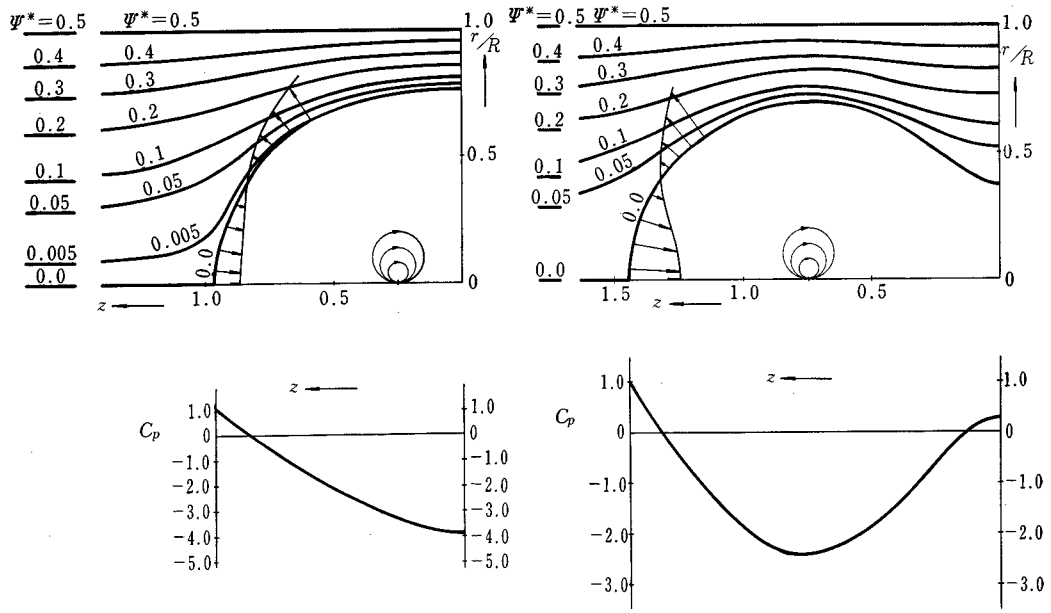

Fig. 10. Karman flow $M/U_m=0.25$, $a/R=0.5$.

Fig. 11. Karman flow $M/U_m=0.25$, $a/R=1.5$.

4. Observation of Flow Patterns

Figure 12 shows the apparatus of observing the streamlines. An alminium plate whose surface is painted out with black color is horizontally placed in a plane including the tube axis. The length of an alminium plate is 250 mm. The tube length is 1,500 mm and the inner diameter is 96 mm. Each half body which is obtained from the stagnation streamline of this analysis is fixed on upper and lower sides of an alminium plate. Air is sent by a blower from left to right in a tube as shown in Fig. 12.

The method used here for observation of streamline is the oil flow pattern.[4] The result obtained from this method is shown in Fig. 13.

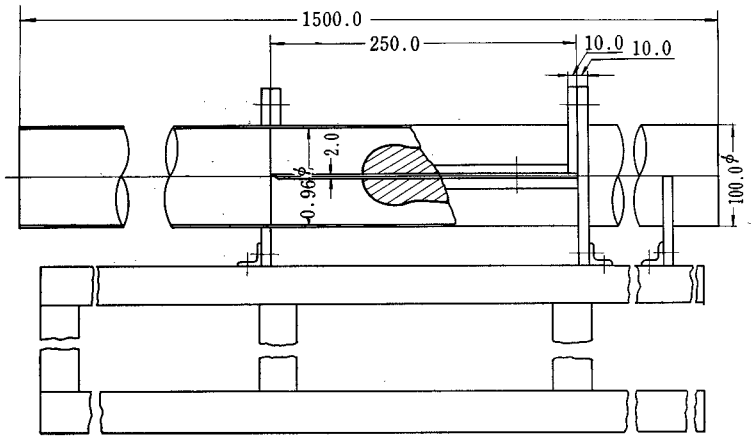

Fig. 12. The apparatus of observing the streamlines.

From the result of the measurement of the velocity profile, it is considered that the upstream flow in a tube is almost Karman flow, so we observed the flow of the case of $M/U_m=0.25$ and $a/R=1.0$ in Karman flow. In this experiment the Reynolds' number specified with the inner diameter of the tube is 1.18×10^5. A pair of vortices grow up in rear of the body due to the separation from body surface as shown in Fig. 13. However, we except that a flow pattern around the front of the body resembles to a calculated flow pattern. But a new streamline yields in front of the stagnation point. This is considered as a new streamline yielded by the separation of the boundary layer on the plate. And also it can be observed that free vortices have generated.

Figure 14 is the case of Reynolds' number $=1.27\times10^5$. In order to extinguish the affection of the boundary layer on the plate, we cut the plate at the stagnation of the body as shown in Fig. 14. And we observe a flow pattern by means of an oil flow pattern at the lee side of the stagnation point and tuft at the wind side of it. It seems that the flow pattern in this way shows almost nearly an actual flow pattern.

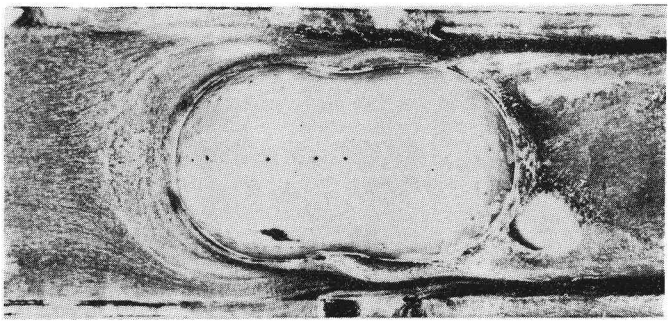

Fig. 13. The streamlines past a body obtained by the oil flow pattern method. Reynolds number specified with the inner diameter of the tube is 1.18×10^5.

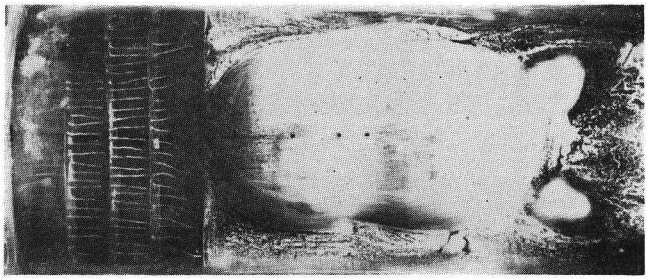

Fig. 14. The streamlines past a body obtained by the tuft method at the front of body and the oil flow pattern method around it. Reynolds number is 1.27×10^5.

5. Concluding remarks

We wish to focus attention on the results of the theoretical calculation of the above mentioned doublet distributions. In any doublet strength and any distance between them,

the pressure coefficient in uniform flow or Karman flow at large blockage ratio due to the affection of the tube wall is much lower than that in shear flow.

It seems that the above tendency is noticeable in one doublet rather than two doublets in the case of the same total doublet strength and is proportional to doublet strength.

In the case of irrotational flow and of rotational flow in a tube, in constructing bodies of arbitrary shape which does not have a sharp nose, we can utilize any or all of the above doublet distributions with superposition.

In the observation of the flow of axially symmetrical bodies, the oil flow method using the plate does not show us the actual flow pattern.

References

1) Philip Levine, J. Aero/Sci., **25**, 33 (1958).
2) Wei Lai, J. Fluid Mech., **18**, 587 (1964).
3) G. K. Batchelor, An Introduction to Fluid Dynamics, Cambridge at the University Press, (1967).
4) Hitoshi Murai, Science of Machine, **23**, 268 (1971).
5) H. Lamb, Hydrodynamics, Dover Publications, New York (1945).
6) Watson G. N., Theory of Bessel Functions, Cambridge at the University Press, (1922).